Available online at www.sciencedirect.com

ScienceDirect

Mendeleev Commun., 2024, **34**, 81–84

Mendeleev Communications

Investigation of methylene blue dye adsorption on nanographite oxide prepared by electrochemical exfoliation

Elena Yu. Obraztsova,* Evgeniy S. Bakunin, Andrey A. Degtyarev, Artem V. Rukhov, Denis V. Obraztsov, Maria S. Goncharova, Inna A. Zhabkina and Alexandra V. Trishina

Tambov State Technical University, 392000 Tambov, Russian Federation. E-mail: nikif83@mail.ru

DOI: 10.1016/j.mencom.2024.01.024

The adsorption properties of nanographite oxide (NGO) prepared by electrochemical exfoliation have been explored using methylene blue (MB) dye. It has been found that NGO adsorbs MB molecules through π–π interaction and proton transfer from the carboxyl group of NGO to the MB molecule. It has been proved that the adsorption process obeys the Freundlich isotherm model and the pseudo-second-order kinetic model, the thermodynamic parameters of which indicate that the process occurs spontaneously, while achieving a dye removal rate of 75 to 98% with a final dye concentration of only 0.005 mg dm^{-3}.

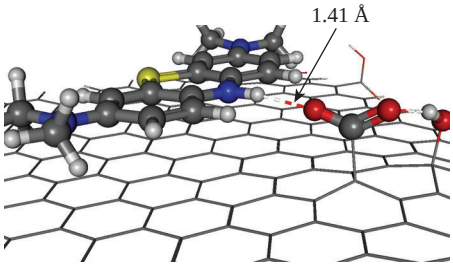

Keywords: nanographite oxide, contaminants, methylene blue, adsorption, isotherm.

Industrial effluents containing dyes are among the leading causes of natural resource pollution, and their treatment remains a major challenge due to the low concentrations of dyes in contaminated natural water and the high cost of their removal. In addition, most of these dyes are toxic, non-biodegradable and harmful to both the aquatic biosphere and humans.[1–3]

Materials developed for the adsorption of dyes from wastewater include a variety of noble metals, metal oxides and carbon-based nanoproducts. Activated carbon is one of the most widely used carbon adsorbents, but its use in wastewater treatment from dyes remains rather an expensive process.[4] At the same time, there is a growing interest in the development of new carbon adsorbents that have the advantages of nanoscale carbon materials, but are less expensive.[5,6] Nanographite oxide (NGO) is a promising material that meets the above requirements. Owing to its two-dimensional structure, developed surface and the presence of functional groups, it can be used as an efficient sorbent for substances of various nature.[7,8]

NGOs are obtained in a variety of ways, among which one of the most popular is the Hummers method and its various modifications,[9,10] which are based on the chemical oxidation of graphite with strong oxidizing agents such as $KMnO_4$, $NaNO_3$, $HClO_4$ and concentrated H_2SO_4. However, this method is very laborious, difficult to control, requires the use of expensive corrosion-resistant equipment and is accompanied by the release of toxic and explosive gases such as oxides of nitrogen, sulfur and chlorine, which makes it difficult to scale up. Currently, one of the promising methods for the preparation of oxidized graphene structures is electrochemical exfoliation of graphite.[11–15] This method is distinguished by its simple hardware design, does not require the use of expensive reagents and is also highly environmentally friendly due to the possibility of organizing a closed production cycle. However, this method has not yet been comprehensively studied, and in the literature there is practically no data on the adsorption capacity of NGO powders obtained by the electrochemical method. The adsorption mechanism, the geometry of the resulting complexes and thermodynamic parameters have not been determined.

For this study, NGO was synthesized by electrochemical exfoliation of graphite foil of the 'Graflex' brand according to the reported method.[16] In the IR spectra of the obtained material, absorption bands are observed in the range of 3000–3600 cm^{-1}, which can be attributed to stretching vibrations of O–H bonds. The absorption band at 1735 cm^{-1} corresponds to vibrations of the C=O bond in ketone or carbonyl groups, the band at 1296 cm^{-1} characterizes the –C–O vibrations of the carboxyl group, and the band at 1164 cm^{-1} is associated with vibrations of the C–OH bond.

A solution of the cationic dye 3,7-bis(dimethylamino)phenothiazin-5-ium chloride (methylene blue, MB) was chosen as a model solution for studying the adsorption capacity of NGO obtained by the electrochemical method.

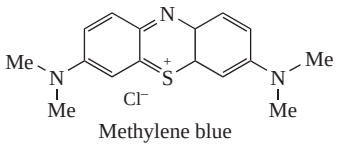

Methylene blue

Figure 1(*a*) shows the adsorption isotherm of MB on NGO powder [equation (S2), see Online Supplementary Materials]. The maximum sorption capacity was found to be 200 mg g^{-1}, which makes it possible to extract from 75 to 98% of MB from the solution, depending on the initial concentration of the dye.

Adsorption isotherms were modeled using the basic equilibrium equations of the Langmuir, Freundlich and Dubinin–Radushkevich isotherm models [equations (S3)–(S5)].

According to the data obtained (Table 1), the adsorption of MB on the surface of NGO is most adequately described by the Freundlich model with an approximation reliability of 0.9995. Consequently, the adsorption occurs on a heterogeneous surface,

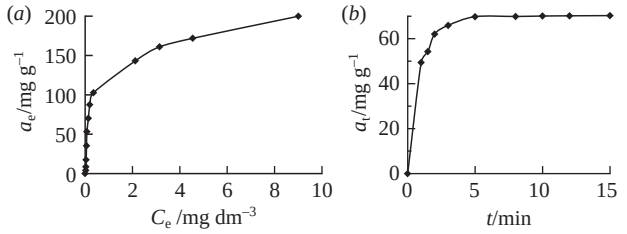

Figure 1 (*a*) Adsorption isotherm and (*b*) kinetic curve for the adsorption of MB on the NGO surface at an initial MB concentration of 4 mg dm^{-3}, temperature 298 K and analytical wavelength 660 nm. Parameters: a_e is the equilibrium adsorption value, a_t is the adsorption value at time t, and C_e is the equilibrium concentration of MB in solution.

where most active centers have different energies. This is apparently due to the presence of different types of functional groups with different degrees of oxidation, located both at the grain boundaries and in the basal plane.

Data processing in the coordinates of the Dubinin–Radushkevich isotherm[18] showed that the activation energy of the adsorption process is about 9.5 kJ mol^{-1}, which indicates the presence of an energy barrier with energy consumption for the formation of a bond, mainly chemical.

Kinetic studies were performed at an initial MB concentration of 4 mg dm^{-3}, an adsorbent mass of 4.5×10^{-3} g and a temperature from 298 to 343 K. The integral kinetic curve of MB adsorption is presented in Figure 1(*b*). According to experimental data, equilibrium in the MB–NGO system is established rather quickly, within 1–5 min. Taking into account the heterogeneity of the processes under study, several kinetic models were used to describe them.

Processing of adsorption kinetic curves [Figure 2(*a*),(*b*) and Table S1, see Online Supplementary Materials] was carried out within the framework of the Lagergren pseudo-first-order model [equation (S8)] and the pseudo-second-order model [equation (S9)].[18]

From the adsorption kinetic curves it is clear [see Figure 2(*a*),(*b*)] that the pseudo-second-order model has a fairly high coefficient of determination $R^2 = 0.992$, which indicates that the chemical reaction limits the sorption process, and the reaction between the sorbate and functional groups occurs in equimolecular ratios and is a second-order reaction. Based on the parameters of the pseudo-second-order equation, the initial adsorption rate [equation (S10)] was calculated to be 0.052 mg g^{-1} min^{-1}.

The shape of kinetic curves indicates the existence of several sorption periods: in the first, short period of time, the rate of cation extraction is the highest, and in the second, the rate is significantly reduced.

To estimate the contribution of internal and external diffusion to the overall rate of the sorption process, experimental kinetic data were processed within the framework of the Boyd–Adamson[19] model [Figure 2(*c*)] and the Weber–Morris[20] model [Figure 2(*d*)].

To calculate external diffusion (transport in solution at the interface with the sorbent), a simplified form of the Boyd–Adamson

Table 1 Constants of the Freundlich, Langmuir and Dubinin-Radushkevich equations.

Equation	Constants[a]					R^2
	1/n	K_F/ dm^3 mg^{-1}	K_L/ dm^3 mg^{-1}	K_{DR}/ dm^3 mg^{-1}	E/ kJ mol^{-1}	
Freundlich	0.282	112				0.9995
Langmuir			1.62			0.9750
Dubinin–Radushkevich				0.028	9.5	0.9987

[a] K_L, K_F and K_{DR} are the constants of the Langmuir, Freundlich and Dubinin–Radushkevich equations, and E is the activation energy.

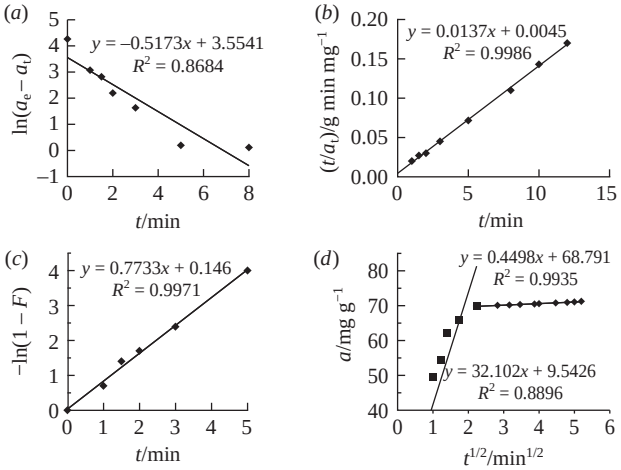

Figure 2 Adsorption kinetic curves in the coordinates of (*a*) the pseudo-first-order model [equation (S8)], (*b*) the pseudo-second-order model [equation (S9)], (*c*) the Boyd–Adamson model [equation (S11)] and (*d*) the Morris–Weber model [equation (S12)].

film diffusion equation [equation (S11)] was used, relating the degree of completeness of the process $F = a_t/a_e$ and the rate constant of external diffusion.

As is known, if the process is limited by external diffusion, the kinetic curve within the Boyd–Adamson model is linear in the coordinates $-\ln(1 - F)$ *vs.* t, and if the limiting stage is sorption in grains, then the linearity of the kinetic curve is observed in the coordinates F *vs.* t. At low degrees of process completion ($F \leqslant 0.8$), experimental data can be adequately described by kinetic curves plotted in the coordinates $-\ln(1 - F)$ *vs.* t, with a reliable approximation value $R^2 = 0.995$–0.998 and passing through the origin of coordinates [Figure 2(*c*)], which indicates a significant influence of the external diffusion stage of mass transfer on the overall adsorption rate at the initial stages. At the final stage, with an increase in the degree of surface coverage, the adsorption curve according to the Morris–Weber model [equation (S12)] becomes linear in coordinates a *vs.* $t^{1/2}$, which indicates the appearance of intra-diffusion constraints.

The thermodynamic characteristics of the adsorption process were determined according to the reported procedure.[17] To estimate the effect of temperature on the adsorption of MB on the NGO surface, we calculated the value of the Gibbs energy (Table 2) using the Van't Hoff equation and equations (S6) and (S7) and determined the entropy and enthalpy of the reaction graphically (Figure S1, see Online Supplementary Materials).

The negative values of the Gibbs energy and enthalpy prove the exothermic and spontaneous nature of adsorption with high affinity of MB to NGO. An increase in the Gibbs energy from −31.47 to −25.31 kJ mol^{-1} indicates that the thermodynamic probability of the sorption process decreases with increasing temperature.

To confirm the theoretical calculations, the sorption of MB on the surface of NGO was modeled through the interaction of a dye molecule with a graphene oxide sheet of 8 × 8 rings (~20 × ~20 Å), decorated with oxygen-containing groups (–COOH and –OH), distributed both along the edges and on the surface of the sheet.

Table 2 Thermodynamic data on the adsorption of MB on the NGO surface.

T/K	ΔG/kJ mol^{-1}	ΔH/kJ mol^{-1}	ΔS/kJ mol^{-1} K^{-1}
298	–31. 47	–73.21	0.1388
313	–29.83		
328	–27.46		
343	–25.31		

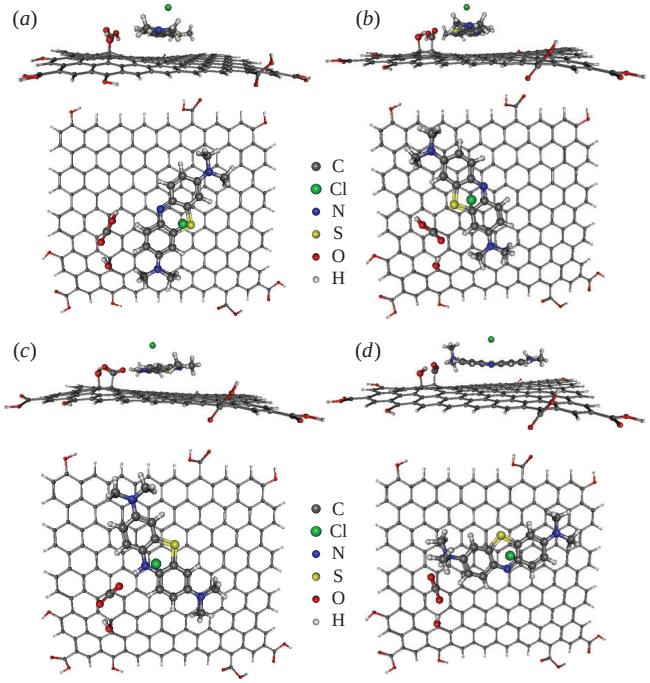

Figure 3 Structure of sorbate–sorbent complexes on the surface of graphene oxide, side view (above) and top view (below): (*a*) complex **1**, (*b*) complex **2**, (*c*) complex **3** and (*d*) complex **4**.

To calculate the geometry and thermodynamic characteristics of sorbate–sorbent complexes, a semi-empirical method based on the density functional theory GFN2-XTB[21] in combination with the ALPB continuum solvation model[22] was used. All calculations were performed in the ORCA 5 software package.[23]

According to the calculation results, all sorbate–sorbent complexes have a geometry in which the MB molecule is located parallel to the plane of the graphene oxide sheet. The distance between the planes of graphene oxide and MB is about 3.2 Å, which is close to the interplanar distance in graphite (3.25 Å).

The appearance of the complexes is presented in Figure 3. The thermodynamic characteristics of sorption are given in Table 3. A total of four complexes were identified. They can be tentatively divided into two types: complexes without changing the chemical structure of the sorbate and sorbent [Figure 3(*a*),(*b*)] and complexes with proton transfer from the carboxyl group of graphene oxide to the MB molecule [Figure 3(*c*),(*d*)].

From Figure 3 it is clear that MB interacts with various functional groups of graphene oxide in different complexes, namely, with the hydrogen atoms of the aromatic ring in complex **1**, with the sulfur atom and hydrogen atom of the aromatic ring in complex **2**, with the protonated nitrogen atom of the heterocycle in complex **3** and with the protonated nitrogen atom of the amino group in complex **4**.

In the complexes without a change in the chemical structure, the main contribution to the sorption energy apparently comes from the interaction of π-orbitals, since the hydrogen bonds between the oxygen of the carboxyl group and the hydrogens of the aromatic ring are weak (the C–H bond has low polarity), and there is practically no interaction with the sulfur atom (distances

Table 3 Calculated thermodynamic characteristics of the formation of MB complexes with the surface of graphene oxide.

Complex	ΔH/kJ mol^{-1}	ΔG/kJ mol^{-1}
1	–118.8	–48.9
2	–131.3	–61.3
3	–218.7	–142.9
4	–116.2	–40.9

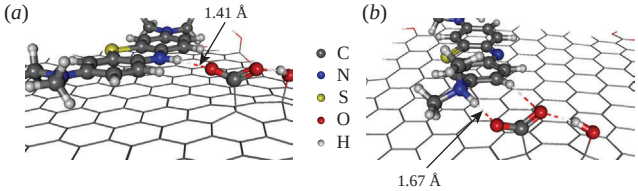

Figure 4 Proton transfer to the MB molecule: (*a*) to the nitrogen of the heterocycle in complex **3** and (*b*) to the aliphatic amino group in complex **4**.

to oxygen atoms are 3.45 and 3.51 Å). The energy of the π–π interaction can be estimated as ~120 kJ mol^{-1}.

For the complexes with a change in chemical structure, additional energy of ~100 kJ mol^{-1} is released due to the proton transfer. In this case, if the transfer occurs to the nitrogen of the heterocycle [Figure 4(*a*)], the overall planarity of the MB molecule is maintained, but if the proton is transferred to the aliphatic amino group [Figure 4(*b*)], then the structure is distorted and some part of the molecule loses planarity with an energy consumption of ~100 kJ mol^{-1}. In all cases with proton transfer, there is a hydrogen bond between the carboxyl group and the hydrogen atom of the MB cation.

Let us estimate the maximum sorption capacity for this mechanism. The area occupied by one molecule is 138.6 Å^2. If we assume that the entire area of the adsorbent is suitable for this mechanism, the limiting value of the adsorption monolayer will be 0.076704 mmol g^{-1} or 24.5 mg g^{-1}. These values can be taken as limiting for monomolecular sorption of the dye parallel to the graphene layers.

Thus, the study of the mechanism of adsorption of methylene blue by nanographite oxide has shown that the latter can efficiently remove this dye from aqueous solutions even at low concentrations. It has been proved that the adsorption process obeys the Freundlich isotherm model and the pseudo-second-order kinetic model. The thermodynamic parameters indicate that the adsorption process occurs spontaneously, thus achieving a methylene blue removal rate of 75 to 98% with a final dye concentration of only 0.005 mg dm^{-3}. It has been found that the adsorption mechanism is based on the interaction of dye molecules with functional groups on the surface of graphene oxide through π–π interactions and proton transfer from the carboxyl group of graphene oxide to the methylene blue molecule. The results obtained can be applied to optimize the conditions for the adsorption of dyes from aqueous solutions, which can be used with high efficiency to remove other dissolved contaminants from aqueous solutions.

This work was carried out within the framework of a grant to support applied research of young scientists in 2022 in the Tambov region (project no. MU2022-02/25).

Online Supplementary Materials

Supplementary data associated with this article can be found in the online version at doi: 10.1016/j.mencom.2024.01.024.

References

1 A. Pala and E. Tokat, *Water Res.*, 2002, **36**, 2920.
2 K.-T. Chung, *J. Environ. Sci. Health, Part C: Environ. Carcinog. Ecotoxicol. Rev.*, 2016, **34**, 233.
3 M. A. Hassaan and A. El Nemr, *American Journal of Environmental Science and Engineering*, 2017, **1**, 64.
4 M. M. Hassan and C. J. Hawkyard, in *Environmental Aspects of Textile Dyeing*, ed. R. M. Christie, Woodhead Publishing, Abington, UK, 2007, pp. 149–190.
5 K. S. Rao, M. Mohapatra, S. Anand and P. Venkateswarlu, *International Journal of Engineering, Science and Technology*, 2010, **2**, 81.
6 I. Sheet, A. Kabbani and H. Holail, *Energy Procedia*, 2014, **50**, 130.

7 D. Shu, F. Feng, H. Han and Z. Ma, *Chem. Eng. J.*, 2017, **324**, 1.
8 T. Ma, P. R. Chang, P. Zheng, F. Zhao and X. Ma, *Chem. Eng. J.*, 2014, **240**, 595.
9 W. S. Hummers, Jr. and R. E. Offeman, *J. Am. Chem. Soc.*, 1958, **80**, 1339.
10 B. C. Brodie, *Philos. Trans. R. Soc. London*, 1859, **149**, 249.
11 C. E. Ibarra Torres, T. E. Serrano Quezada, O. V. Kharissova, H. Zeng, B. I. Kharisov, E. Luevano Hipólito, L. M. Torres-Martínez and L. T. González, *Mendeleev Commun.*, 2023, **33**, 572.
12 V. P. Vasiliev, R. A. Manzhos, A. G. Krivenko, E. N. Kabachkov and Y. M. Shulga, *Mendeleev Commun.*, 2021, **31**, 529.
13 D. V. Chernysheva, I. N. Leontyev, M. V. Avramenko, N. V. Lyanguzov, T. I. Grebenyuk and N. V. Smirnova, *Mendeleev Commun.*, 2021, **31**, 160.
14 A. B. Kuriganova, I. N. Leontyev, M. V. Avramenko, N. A. Faddeev and N. V. Smirnova, *Mendeleev Commun.*, 2022, **32**, 308.
15 E. S. Bakunin, E. Yu. Obraztsova and A. V. Rukhov, *Inorganic Materials: Applied Research*, 2019, **10**, 249 (*Perspekt. Mater.*, 2018, no. 7, 5).
16 E. Yu. Obraztsova, A. A. Degtyarev, A. V. Rukhov and E. S. Bakunin, *Vestn. Tambov. Gos. Tekh. Univ.*, 2019, **25**, 116 (in Russian).
17 A. A. Khan and R. P. Singh, *Colloids Surf.*, 1987, **24**, 33.
18 M. M. Dubinin and L. V. Radushkevich, *Dokl. Akad. Nauk SSSR*, 1947, **55**, 327 (in Russian).
19 G. E Boyd, A. W. Adamson and L. S. Myers, Jr., *J. Am. Chem. Soc.*, 1947, **69**, 2836.
20 W. J. Weber, Jr. and J. C. Morris, *J. Sanit. Eng. Div., Am. Soc. Civ. Eng.*, 1963, **89** (2), 31.
21 C. Bannwarth, S. Ehlert and S. Grimme, *J. Chem. Theory Comput.*, 2019, **15**, 1652.
22 S. Ehlert, M. Stahn, S. Spicher and S. Grimme, *J. Chem. Theory Comput.*, 2021, **17**, 4250.
23 F. Neese, *Wiley Interdiscip. Rev.: Comput. Mol. Sci.*, 2022, **12**, e1606.

Received: 2nd June 2023; Com. 23/7181